Journal of Studies in Science and Engineering

EngiScience Publisher

Research Article

Investigation of Strengthening Reinforced Concrete Beam-Column Connection Wrapped with Fiber-Reinforced Polymer

Rzgar A. Mohammed [1,*], Hersh F. Mahmood [2]

[1] Civil Engineering Department, University of Raparin, Sulaimani, 46012, Iraq

[2] Civil Engineering Department, University of Halabja, Halabja, 46018, Iraq

*Corresponding Author: Rzgar A. Mohammed, E-mail: rzgar.asad@uor.edu.krd

Article Info

Article History

Received Jan 27, 2022

Revised Mar 01, 2022

Accepted Mar 11, 2022

Keywords

Beam to column joints,
Finite element software
CFRP sheet

Abstract

In reinforced concrete structures, the beam-column connection area has a considerable influence on the behavior of the structure. The use of fiber-reinforced polymer FRP to strengthen the connections in the Reinforced structure can be one of the solutions to transform this area, thus improving the behavior of the structure, which is achieved through the use of fiber-reinforced polymer of carbon to achieve high-strength concrete beam-column connections Investigations have been conducted using finite element modeling. The concrete damage plasticity model has been used to analyze the model. The results show that the bearing capacity has developed considerably, but the ductility is also significantly reduced. The study also evaluated the qualities of various reinforcement models and proposed the most effective reinforcement model. The use of fiber-reinforced polymer in the flex zone with fibers oriented at forty-five degrees in the shear zone of the joint showed the most significant changes in behavior. The demolition of reinforced concrete beam-column joints is a sudden failure without prior notice, since the collapse of the column and the connection before the break of the beam are undesirable, their occurrence can cause irreparable damage.

1. Introduction

The construction industry can use various types of reinforcement materials, such as steel plates, cement, and fiber-reinforced polymers, to coat the affected parts, the most common being steel coating [1]. These types of jackets increase the weight and size of the structural elements. Some attempts to use a corrugated steel plate or an ordinary steel plate as a facing material in the concrete frame [2]. Compared with other materials, FRP-based reinforcement has become attractive due to its lightweight, high strength, and rigidity, corrosion resistance, easier implementation, excellent fatigue, etc., and is an attractive alternative to restore the together to your required capacity. According to Gergely et al. [3] , CFRP composite materials can increase the strength, ductility, and shear strength of beam-column joints. Mukherjee and Joshi [4], found that GFRP and CFRP can be used for earthquake repair and the repair of reinforced concrete joints. Pentelides et al. [5] concluded that the shear capacity of beam-column joints increased by 35% with the use of composite materials. Ghobarah and ElAmoury [6] found that the use of CFRP rehabilitation technology can effectively prevent fragile joints from shearing and joint slippage. Turangi et al. [7] The maximum load of the CFRP-modified beam was found to be 170% greater than that of the control beam. Kachlakev and McCurry, [8] also found that beams reinforced with CFRP and GFRP laminates have increased their bending and shear capacities by more than 150%. Antonopoulos and Triantafillou [9] studied the role of various forms of FRP composite plates, sheets, and rods in structural reinforcement, and discussed their role in improving the shear ability of joints. Karayannis and Sirkelis [10], used a combination of epoxy resin injection and CFRP plates and found that the bearing capacity, ductility, and energy absorption of the beam-column joints were significantly improved. [11]observed that CFRP-reinforced beams exhibit higher stiffness and retarded tensile cracking under higher loads. In the case of beams reinforced with CFRP bonded laminates, significant flexural and shear reinforcement has been observed D`Ayala et al. studied FRP fabrics with different designs and adhered to RC beam and column nodes, and found that the reinforcement procedure increased stiffness and ductility while increasing shear and bending strength and dissipation [12].

2. The Objectives and Purposes of Research

Because the joints of the corner frame are one of the most important components of concrete structures with bending and the lack of sufficient capacity and ductility in the connection area can lead to a failure of the joints and , consequently, the loss of strength and overall failure structures. the bond performance between FRP and surrounding concrete can be improved using mechanical anchorages such as surface deformations and sand coating. During strong ground motion and dynamic loading, the lower ductility of FRP still is a major concern, steel-reinforced and FRP reinforced beams behave similarly in terms of section mechanics. Steel reinforced concrete strength design method applies to that of FRP reinforced beam to find the ultimate moment capacity. However, deflection and ductility criteria govern the design process for FRP reinforcement, which is not the case for steel reinforcement. Lower ductility of FRP remains a major concern, especially in structures subjected to dynamic loading. FRP fails within its elastic range with low energy dissipation capacity, which is considered a major drawback in seismic design. The highlight-strength create is increasingly used, and the engineers are simply following the existing rules with little attention given to the provision of sufficient ductility. Now, it is urgent to develop appropriate rules for the ductility design of the HSC members. For this reason, several kinds of research in recent years have studied the effects of various parameters on the local ductility of HSC members as the concrete strength, the yield strength of steel, and the ratios of tension and compression reinforcement, consequently many methods and formulations to deduce the curvature ductility factor are proposed.

Most of the limited research has been made of reinforced concrete joints, each with a limited number of joints. On the other hand, due to the lack of research into the use of CFRP to render and formulate the HSC-made joints, the reason for this research is to study the strength and ductility of the beam-to-column connection made with Reinforced concrete with CFRP.

The main objectives of this research can be summarized as follows:

1. Considering the column joints in buildings constructed with HSC and retrofitted with CFRP.
2. Effectiveness of CFRP sheets for strengthening of being beam-column joints, especially in seismic areas.
3. Study ductility of the beam-column joints in HSC buildings.
4. Effect of thickness and configuration of CFRP sheets on thebe beam-column section
5. Considering length beam-beam-column joints in buildings constructed of HSC and retrofitted with CFRP.
6. Effectiveness of CFRP sheets for strengthening of being a beam-column job, it's especially in seismic areas.
7. Study ductility of the beam-column joints in HSC buildings.
8. Effect of thickness and configuration of CFRP sheets on the be beam-column section.

3. Method of Research

The present study is a numerical analysis method and its verification is performed by comparing experimental samples so that the results of the experimental work presented in the previous research are used. The research steps are carried out in such a way that first enough studies are carried out in all fields related to the subject matter and the information about the experimental samples and the results obtained from them for the verification of the total work is being developed.

In this study, high-strength concrete (HSC) is used in modeling instead of the conventional concrete used in the laboratory to make connections. The simulated samples are also analyzed once again by CFRP. Finally, the finite element analysis results of CFRP and CFRP connections are compared with laboratory results. The results include the final load of the samples and their shape. The stages of research can be categorized as follows:

1. literature review of the subject.
2. Selection of laboratory samples.
3. Using programming the Abaqus software package and verification of the finite element simulations based on the previous experimental studies.

4. Parametric study
5. Analysis and discussion of results.
6. Compelling and writing thesis.

3.1. Samples Studies

3.1.1. Sample one

Sample one used in this study is connecting the beam to the concrete column of the one-side. Samples were selected according to laboratory samples tested by Khaloo, AS, Dariibi in 2014. The compressive strength of all specimens in the laboratory is 20 MPa. In this study, high-strength concrete is used in analyzes. So that the cross-section dimensions of the columns and beams are equal to 225x125 mm. The length of the beams is 500 millimeters and the height of the columns is equal to 1 meter.

In this study, external reinforced concrete beam-column connections were poured with M20 grade concrete and Fe500 grade steel, as shown in Figure 1. Comply with IS: 10262198, the cement: sand: aggregate ratio is 1: 1.43: 2.97 and the water-cement ratio is 0.48. These beam-column connections were tested by the load arrangements and available test facilities [13]. These beam-column joint samples are 225mm-125mm column cross-sections with a total length of 1000mm and 125mm-225mm cantilever beams with a length of 500mm. The size of the cross-section of the beam is determined as a function of the beam's effective depth/shear span ratio, that is, a / d greater than 2, so it should not act as a bracket/support. In the current situation, the section of shear a, that is, the distance between the point of application of the load and the support, is 450 mm and the effective depth d of the beam is 195 mm.

Therefore, the a / d ratio in this study is 2.3, which is greater than 2. For the nine specimens, four bars with a diameter of 10 mm are provided as longitudinal bars and transverse ties with a diameter of 6 mm, with a separation of 100 mm in the c / c column. The beam is designed as a lightly reinforced section, so two bars with a diameter of 10 mm are provided as tension bars and two bars with a diameter of 8 mm as compression bars and a diameter of 6 to 100 mm c / c. Vertical stirrup mm IS 456: 2000 [14]. Among the nine samples, three were used as control samples and loaded into the final failure load, and the corresponding data were recorded through the data acquisition system.

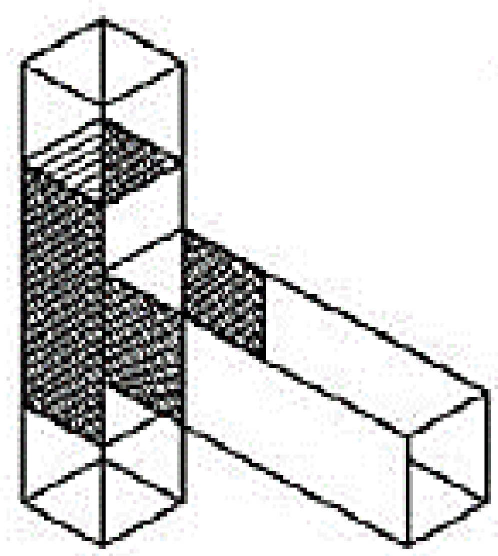

Figure 1. Shear strengthening using 1- and 2 layers of CFRP

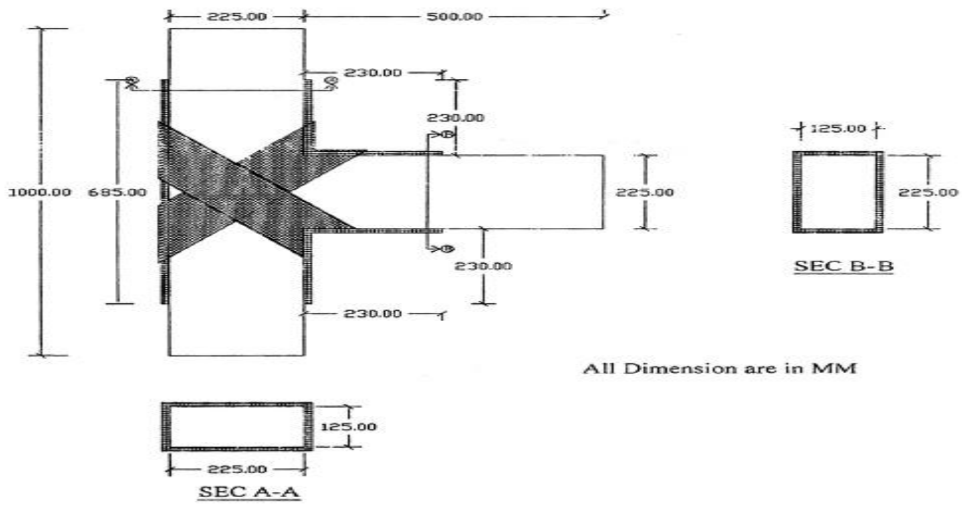

Figure 2. Geometric Properties of the Joints and Details of Their Reinforcement with CFR

Table 1. Mechanical properties of concrete mixer

Ingredent	Quantity
Cement (ppc)	395.62
F.A.	571.63
C.A-I (10mm)	1163.70
CA.II(20mm)	------
Water	189.9

Table 2. Mechanical properties of steel

S.diamete of bars NO. mm	Yield ststrengthing Mpa	Ultimate strength Mpa	Elongation %
1-	554	670	20.5
2-	557	676.23	25.8
3-	442.42	612.70	32.7

Table 3. Specifications of the fibers used to reinforce the joints

Sr.No.	Physical properties	Value
1-	Tensile strength	3800 Mpa
2-	Modulus of elasticity	240 Gpa
3-	Density	1.7 g/cm^3
4-	Stitch	200 gsm
5-	Stitching	230 gsm
6-	Thickness	0.117 mm

3.2. Modeling and Analysis of Samples in Abaqus

Abaqus is one of the most powerful computer-aided engineering soft software finite element analysis. Abaqus can solve problems from simple linear analysis to the most complex nonlinear modeling. This software has a very wide range of elements; any type of geometry can be modeled by these elements. It also has a lot of behavioral patterns. In this research, this software has been used to analyze the connections of this software. The steps of modeling and analyzing samples are presented below.

1. Formation of the model: Modeling of samples in Abaqus is such that different parts of the model, such as rebar, raw material, concrete, and CFRP plates, are separately modeled and, in later stages, these parts assembler.
2. Definition of materials in this step, the specification of materials including concrete, steel, and CFRP should be defined. Specifications of materials include density, modulus of elasticity, compressive strength, and tensile strength of concrete, CFRP, and steel. To determine the mechanical properties of CFRP in Abaqus, the values given in the sample section are used. Popovic's behavioral model for pressurized concrete has been used for reinforced concrete and Romberg for steel to define the characteristics of materials in the plastic ring

3.2.1. Popovic's behavioral model

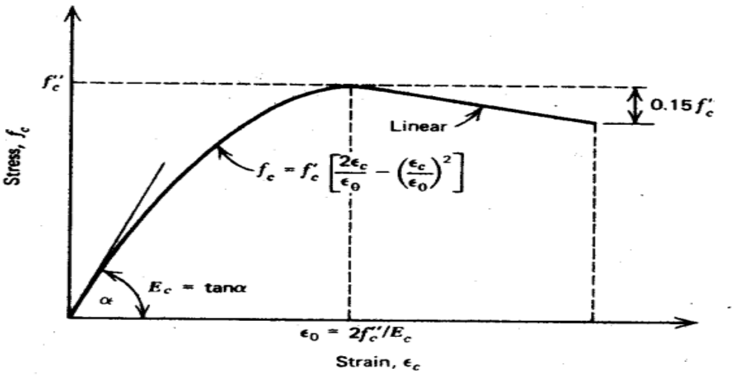

Figure 3. Pressure behavior curve of concrete according to Popovich's proposed relationship

$$\sigma_c = f_c \frac{n\left(\frac{\varepsilon_c}{\varepsilon_{co}}\right)}{n - 1 + \left(\frac{\varepsilon_c}{\varepsilon_{co}}\right)^{nk}} \tag{1}$$

In the upper case, σ_c, f_c, and ε_c are compressive stress, compressive strength, and compression strain, respectively, and the parameters n, k, ε_c,o, and E are obtained from equations (2) to (6).

$$n = 0.8 + \frac{f_c}{17} \tag{2}$$

$$k = 1 \quad \text{if} \quad \varepsilon_c \leq \varepsilon_{co} \quad k = 0.67 + \frac{f_c}{62} \quad \text{if} \quad \varepsilon_c > \varepsilon_{co} \tag{3}$$

$$\varepsilon_{co} = \left(\frac{f_c}{E_c}\right)\frac{n}{n-1} \tag{4}$$

$$E = 5000\sqrt{f_c} \quad \text{if} \quad fc < 50 \text{ mpa} \tag{5}$$

$$E = 3300\sqrt{f_c} + 6900 \quad \text{if} \quad f_c > 50 \text{ mpa} \tag{6}$$

3.2.2. Behavioral model of baby and wachso

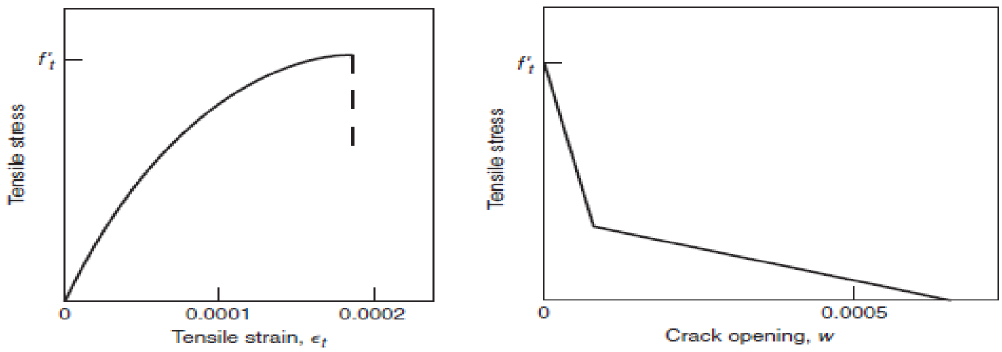

Figure 4. Concrete tensile behavior curve

$$\varepsilon = \frac{\sigma}{E} + \alpha \frac{\sigma}{E}\left(\frac{\sigma}{f_y}\right)^{n-1} \tag{7}$$

$$\alpha = K \left(\frac{f_y}{E}\right)^{n-1} \tag{8}$$

In the above relation, ε, σ, E and F_y respectively represent the strain in steel, the stress in steel, the steel elastic modulus, and the characteristic steel resistance. K and n describe the constants related to the materials used and the hardening behavior of the materials. In this stage, the assignment of the materials defined to the model as well as the definition of the cross-section of the elements of the joints is also carried out.

1. Assembly of the model: At this stage, all parts that are individually defined in the first stage are assembled and form the main model.
2. Define steps and type of analysis: In the definition of the analysis stages, the analyzes of the definition and the desired outputs, such as stress, strain, force, displacement, etc., are specified. The type of analysis is define both the type of loading and output desired. In this research, the Riks analysis is used and the outputs are for changes and changes.
3. Defining Constraints between Materials (Interaction)

The constraints between the contact surfaces of various materials are defined at this stage. In the analysis of the samples, the boundary between the outer surface of the rebar and its surrounding concrete as the Embedded Region and the boundary between the outer surface of the concrete and the surface of the CFRP plates are defined as Tie.

4. Results and Discussion

In the developed 3D FE models, the concrete beam-column connection, the embedded longitudinal and shear reinforcement bars are modeled explicitly. Figure 5. shows that the RC joints were modeled as 3D geometric entities.

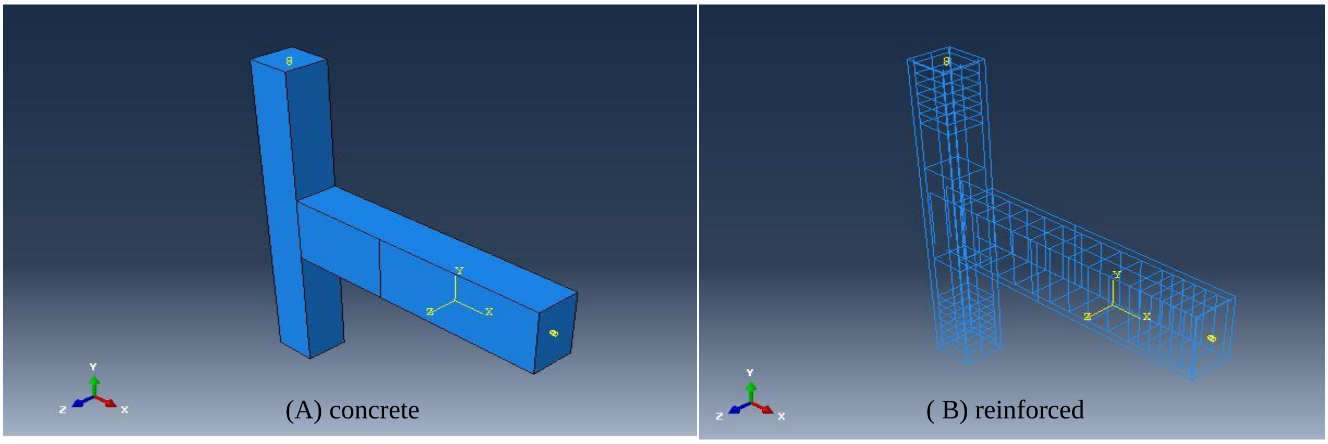

Figure 5. Geometric model of the test specimen

4.1. Mesh

Structured meshing was adopted for all of the solid elements used in the models, as matrices based on structured meshing are simple and fast to assemble. Furthermore, the aspect ratios of solid elements were kept as close to one as practicable, as high aspect ratio elements would affect the accuracy of the analysis. Mesh convergence studies were conducted to determine the best balance between accuracy and computational cost. four element sizes, namely 11 mm, 30mm, 20 mm, and 50 mm, were considered and a uniform element size of 11 mm for model one and 20 mm for model two was finally selected as stated in Section (A), where the validation of the model is discussed. The meshing adopted for all specimens is shown in the Figure 5.

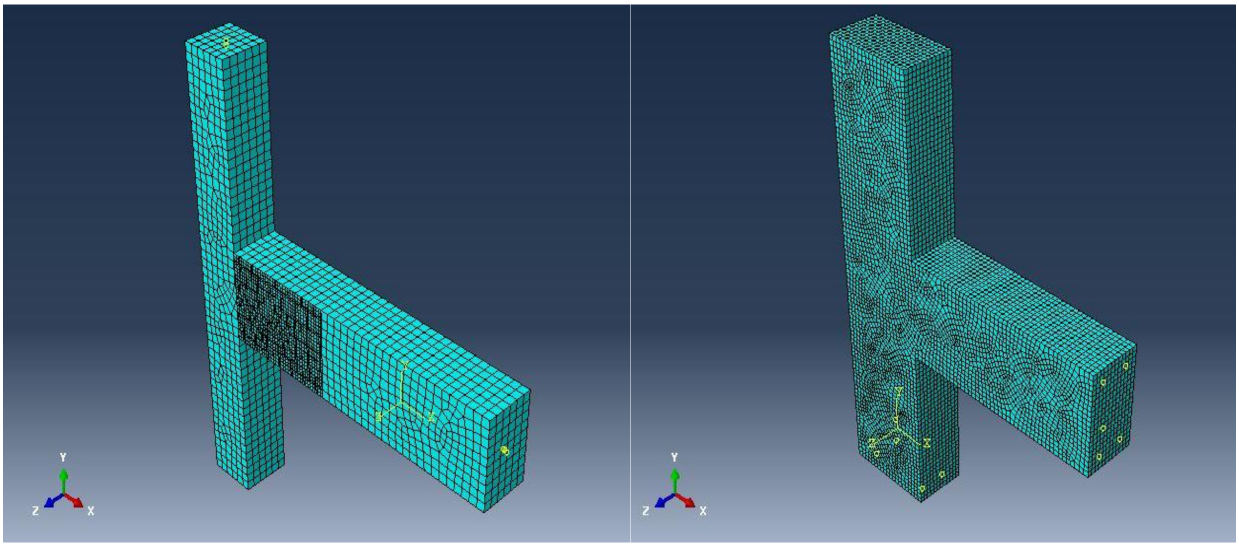

Figure 6. Finite element mesh for two models

4.2. Validation

Perform a mesh convergence study to verify the appropriate mesh size and appropriate material parameters, which are highly consistent with the response observed in the experiment. Initially, four-cell sizes, namely 11mm, 20mm, 30mm, and 50mm were used as the uniform grid size; The results were obtained for each grid, according to the load obtained from the repeated control sample. Response to displacement (Using 11mm and 20mm element sizes) are closer to the experimental results in terms of maximum load and stiffness under maximum load. The similarity of the curves shows that the results of the experimental observation are quite consistent with the predicted results obtained by the finite element analysis using the 11 mm element size sample 1 and the 20 mm element size sample 2.

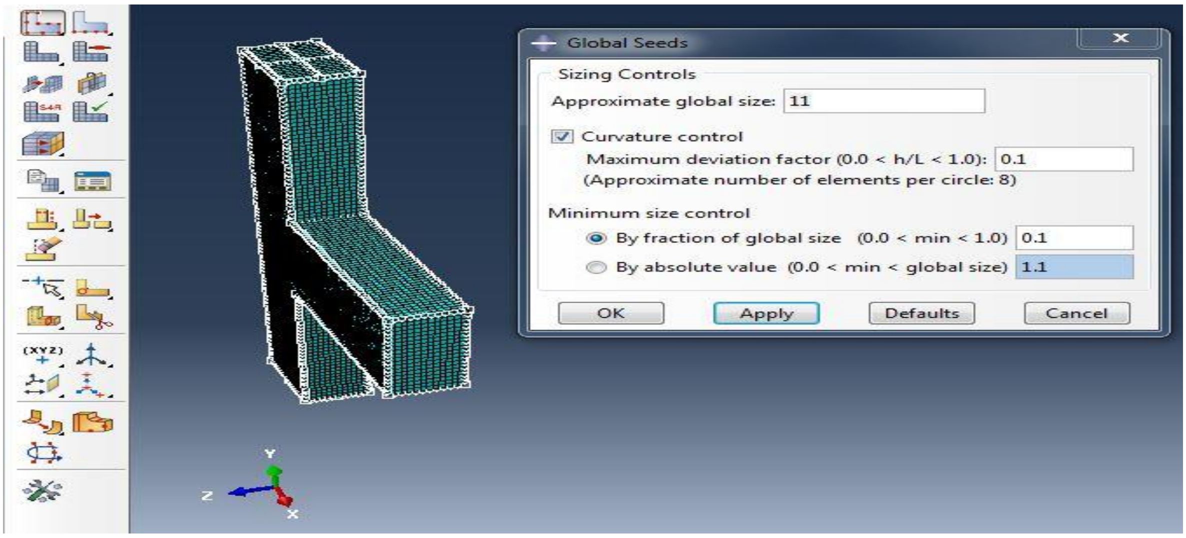

Figure 7. Mesh size for control specimen one

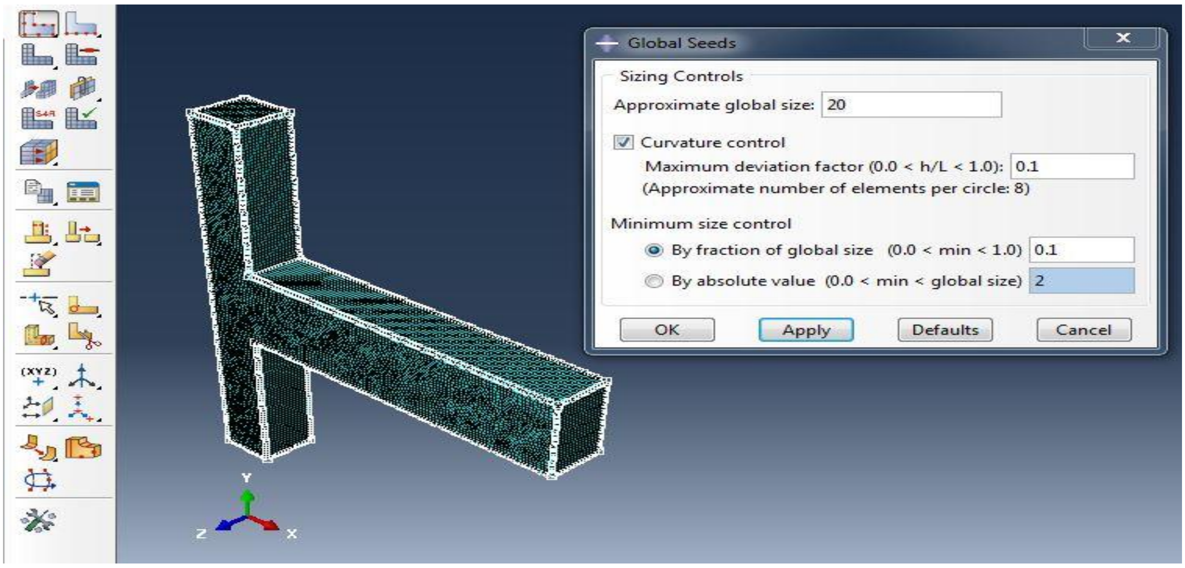

Figure 8. Mesh size for control specimen two

This curves below are verification for normal strength concrete with and without CFRP

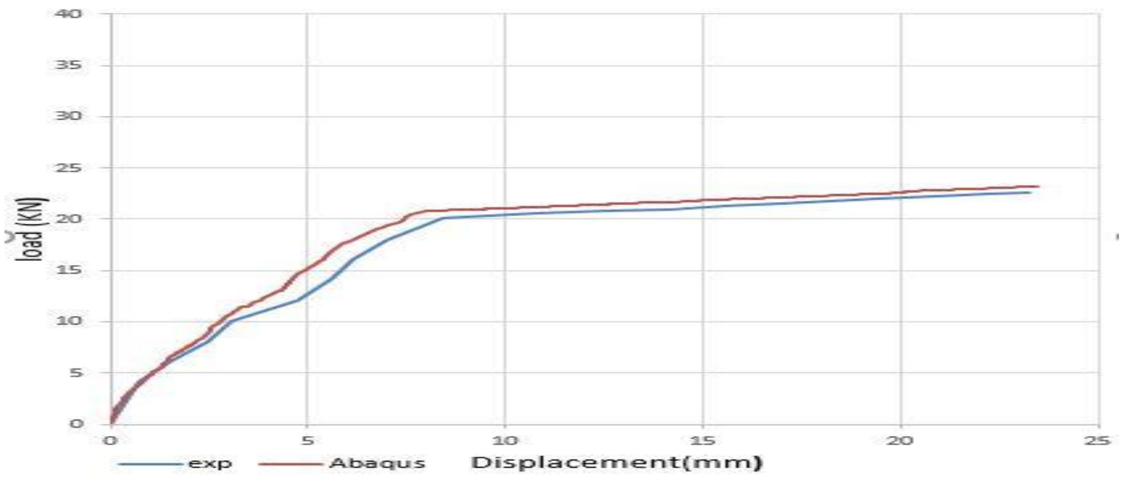

Figure 9. Load-displacement response for normal strength concrete: element size is 11 mm without CFRP

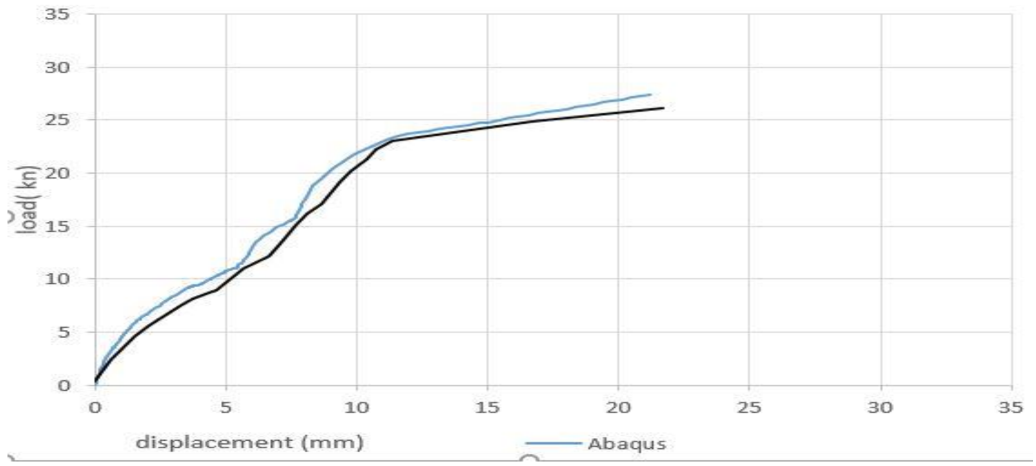

Figure 10. Load-displacement response for normal strength concrete: element size is 11 mm with CFRP

4.3. Verification of Sample Two with HSC Concrete Grade 80 MPa and with Using CFRP.

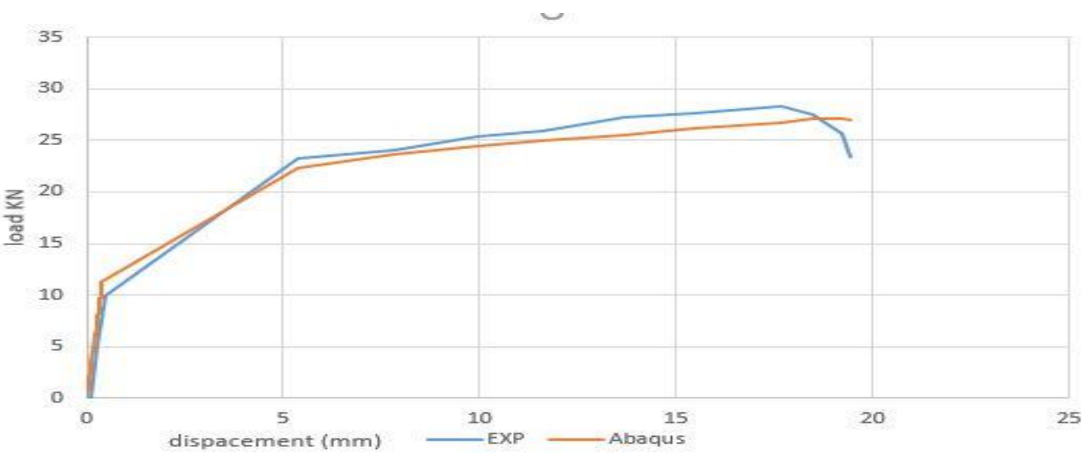

Figure 11. Load-displacement response for High strength concrete and element size is 20 mm

The FE analysis results for the formation of cracks under uniaxial loading compared to those of the experiment. During the experiment, diagonal joint cracks were observed at a load of 23.4 kN for normal strength concrete without CFRP and load 27.1 KN for the sample with CFRP and the ratio for the first Abaqus curve compare to sample is % 1.35 and the second curve is %1.5, and then for the second sample with grade concrete of 80 MP, cracks observed at load 25.3 KN For the CDP concrete material model adopted in the FE analysis, cracking propagation can be visualized by plotting the plastic strain (PE) in the first principal direction (i.e. corresponding to tensile plastic strain). Figure 11 shows this.

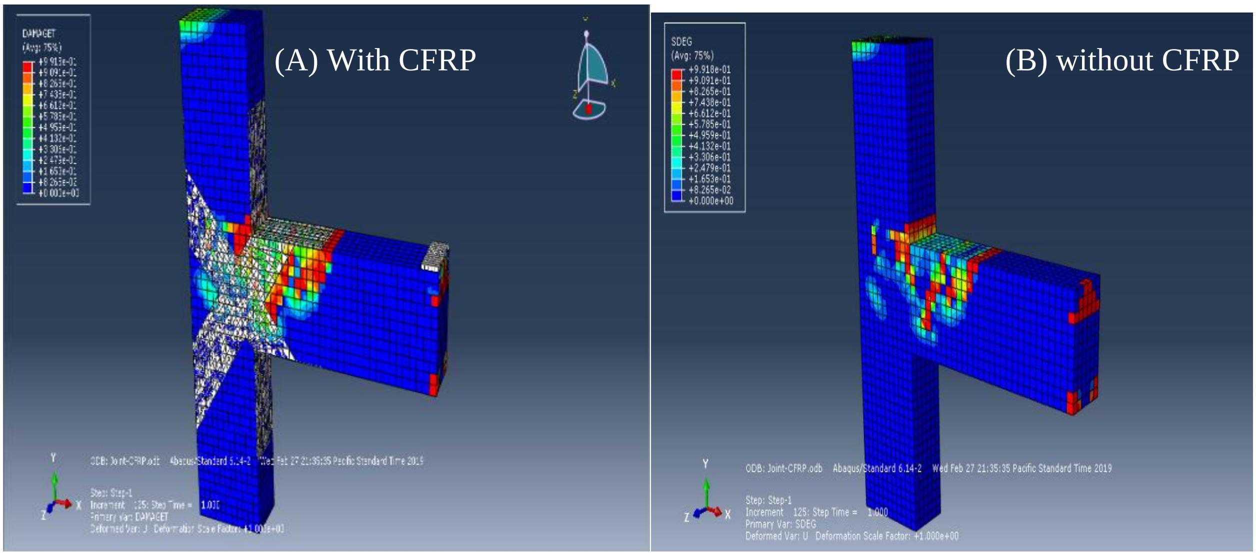

Figure 12. Comparison of crack propagation

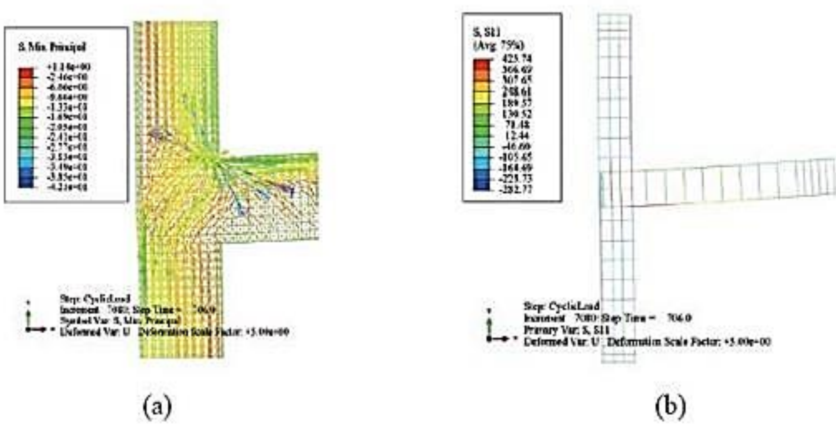

Figure 13. (a) Principal compressive stress in concrete; (b) Tensile stress in reinforcement

The inspection of Figure 12 and 13 explains that the damage mechanism results in the EF analysis are mainly formed in the joint area and identified as shear cracks because most of the main tensile deformation of concrete is concentrated in the slab area. In general, it can be concluded that the model developed using ABAQUS software successfully predicted the failure mode because it is consistent with the failure mode given by the experimental results. Referring to Table 4) the load ratio extracted from the EF analysis is compared with the experimental results.

Table 4 Experiment and FE ultimate load comparison results for every two specimens

Samples	Experiment (KN)	FE (KN)	FE/TEST
1-without CFRP	22.68	23.4	1.031
1-with CFRP	25.4	27.1	1.066
2-with CFRP	26.5	25.3	0.954

Joint behavior is complex and essential for all structural behaviors. Brittle behavior must be avoided for ductile failure mode to become dominant.

- The F.E. developed produces realistic and accurate results and captures joints' complex and non-linear behavior. The model contains most types of nonlinearity, including plastic damage and nonlinear contact behavior, and geometric nonlinearity in concrete.
- Use CFRP to wrap joints, beams, and columns to transform brittle failure into ductile failure. However, CFRP does not work when the model reaches maximum clamping due to beam stirrups or a failure that occurs in the joint. On the other hand, the CFRP envelope effect is important for models that are dominated only by the shear failure of the beam.
- CFRP reinforcement method for beam-column joints severely affected by the initial design. Poor design may enhance the mobility of both; using CFRP's load-bearing capacity and ductility.
- The results show that the uniformity of the stirrups in the joint improves the bearing capacity and ductility of the model dominated by shear failure. This behavior also occurs in the CFRP model, but the ductility is slightly increased.
- As the relative stiffness ratio decreases, the ultimate bearing capacity increases, and the ductility decrease. This trend also exists in the case of using CFRP.
- The ductility increases with the increase of the cross steel, reaching a certain maximum value (Av / s) B, which can be called a fixed value. Increasing (Av / s) B beyond this maximum will not have a significant impact on ductility. This value depends on the relative inertia (G) and the number of stirrups in the joint (Av / s) J. This tendency does not occur when using CFRP, because the use of CFRP converts

brittle failure into ductile failure. It can be seen from the table below that (M1, M2, and M3) do not use CFRP sheeting around the joints and (M4 and M5) use CFRP sheeting around the joints and compare the results.

Table 5. Comparison of displacement between finite element and experimental results

Models	Conditions	Experiment		Finite element		FE/test	FE/Test
		Load (KN)	Displacement Mm	Load (KN)	Displacement mm	Load (KN)	Displacement mm
M1	Without CFRP	22.68	23.24	27.1	21.62	0.95	0.93
M2	Without CFRP	22.68	23.24	32.76	18.21	1.44	0.78
M3	Without CFRP	22.68	23.24	34.74	16.77	1.53	0.72
M4	With CFRP	25.4	22.66	35.36	27.3	1.39	1.2
M5	With CFRP	25.4	22.66	44.53	28.7	1.75	1.26

Table 6. Shows an increase in ductility by adding of CFRP layers.

Models	Ultimate Load(KN)	Thickness of CFRP layers	Parametric study Fc: concrete strength in Mpa.	Displ. At yield point	Displ. At ultimate load	ductility
One	27.103	---	Fc=55 Mpa without CFRP	15.7	21.62	1.36
Two	32.76	---	Fc=65 Mpa without CFRP	13.5	16.40	1.2
Three	34.74	---	Fc=70Mpa without CFRP	13.21	15.77	1.12
Four	35.36	0.117	Fc=60Mpa with 1 layer Of CFRP around joint	13.5	27.30	2.02
Five	44.53	0.234	Fc=75Mpa with 2 layer Of CFRP around joint	13	28.70	2.207
Six	30.38	0.117	Fc=80Mpa with 1 layer Of CFRP around joint	10.4	19.6	1.88
Seven	28.96	1	Fc=60Mpa with 1 layer Of CFRP around beam	7.065	21.02	2.97
Eight	31.98	2	Fc=70 Mpa with 2 layer Of CFRP around column	6.56	20.08	3.06
Nine	32.34	3	Fc=75Mpa with 3 layer Of CFRP around joint	5.43	23.52	4.33
Ten	38.85	4	Fc=80Mpa with 4 layer Of CFRP around joint	4.75	22.20	4.67
Eleven	28.88	2	Fc=60Mpa with 2 layer Of CFRP around beam	7.58	20.05	2.64
Twelve	28.3	1	Fc=60Mpa with 1 layer Of CFRP around column	6.59	16.21	2.45

The collapse of many concrete structures that submit the seismic movement gives us the idea of an unwanted design of energy dissipation in the plastic field. In an area of high seismic activity, ductility is an important factor in the design of reinforced concrete elements to guarantee structural integrity within plasticity, where the structure allows the dissipation of seismic energy. Under the seismic load, the structure can dissipate seismic energy by promoting the exposure of the plastic hinges on the beam instead of a column that compares normal concrete and high strength concrete, and the latter is different, has the advantage of providing a very high resistance.

They are shown from table 7. by using CFRP sheets and increasing layers of CFRP the ultimate load-bearing capacity and ductility also increase.

Table 7. Compares results of finite element and experimental due to increase of axial load

Models	Ultimate Load (KN)	Thickness of CFRP layers	Parametric study Fc: concrete strength in Mpa.	Displ. At yield point	Displ. At ultimate load	% increase in axial load FE/ test
One	27.103	---	Fc=55 Mpa without CFRP	15.7	21.62	4.42
Two	32.76	---	Fc=65 Mpa without CFRP	13.5	16.40	6.74
Three	34.74	---	Fc=70Mpa without CFRP	13.21	15.77	8.11
Four	35.36	0.117	Fc=60Mpa with 1 layer Of CFRP around joint	13.5	27.30	12.68
Five	44.53	0.234	Fc=75Mpa with 2 layer Of CFRP around joint	13	28.70	14.4
Six	30.38	0.117	Fc=80Mpa with 1 layer Of CFRP around joint	10.4	19.6	3.38
Seven	28.96	1	Fc=60Mpa with 1 layer Of CFRP around beam	7.065	21.02	1.46
Eight	31.98	2	Fc=70 Mpa with 2 layer Of CFRP around column	6.56	20.08	4.97
Nine	32.34	3	Fc=75Mpa with 3 layer Of CFRP around joint	5.43	23.52	6.34
Ten	38.85	4	Fc=80Mpa with 4 layer Of CFRP around joint	4.75	22.20	8.85
Eleven	28.88	2	Fc=60Mpa with 2 layer Of CFRP around beam	7.58	20.05	1.88
Twelve	28.3	1	Fc=60Mpa with 1 layer Of CFRP around column	6.59	16.21	1.25

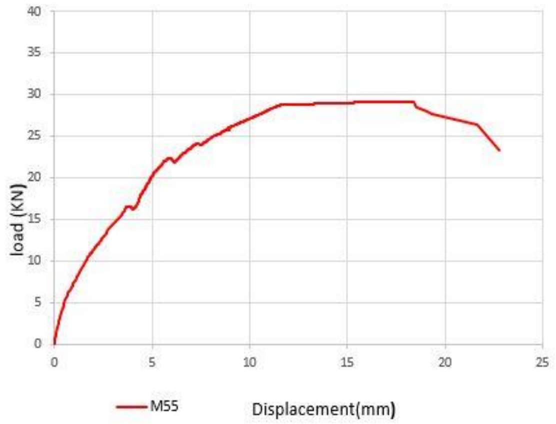

(A)Model one ƒc =55 MPa

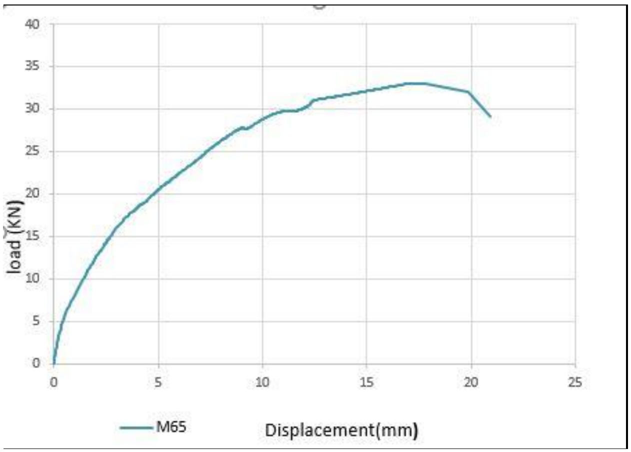

(B) Model two ƒc =65 MPa

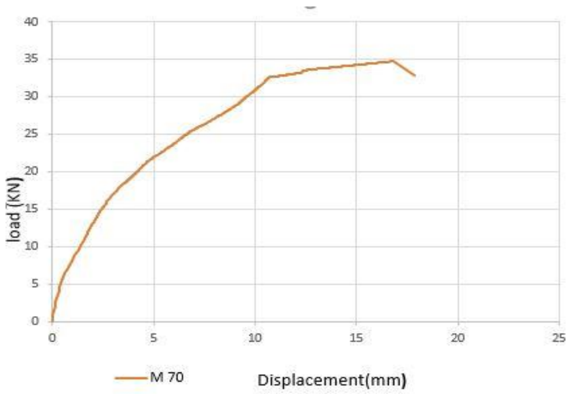

(C) Model three ƒc =70 MPa

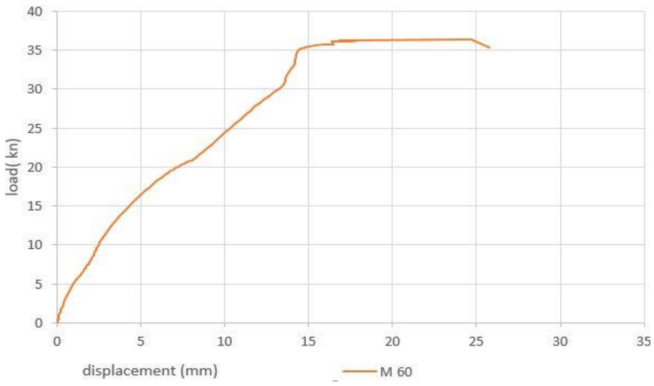

(D) Model four ƒc =60 MPa

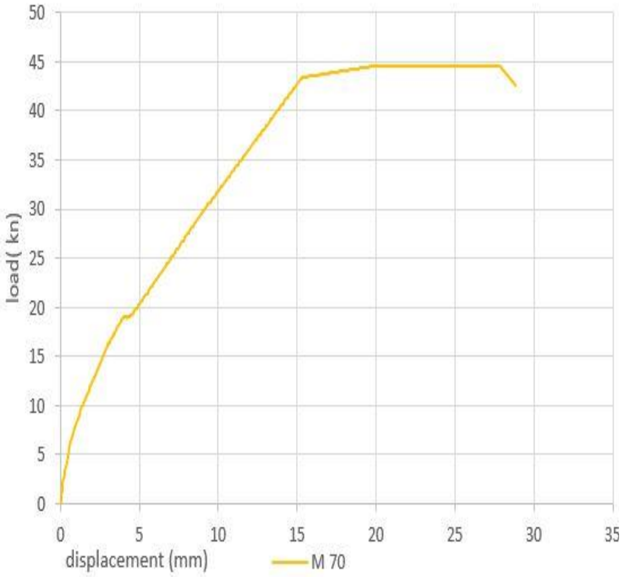

(E) Model one ƒc =75 MPa

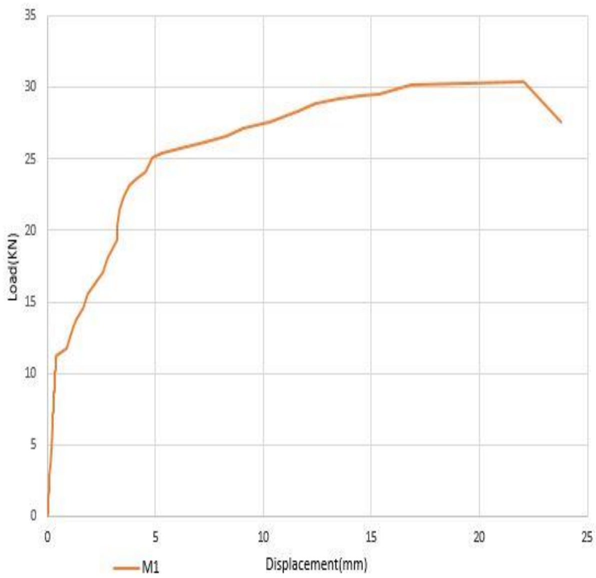

(F) using one layer of CFRP around joint

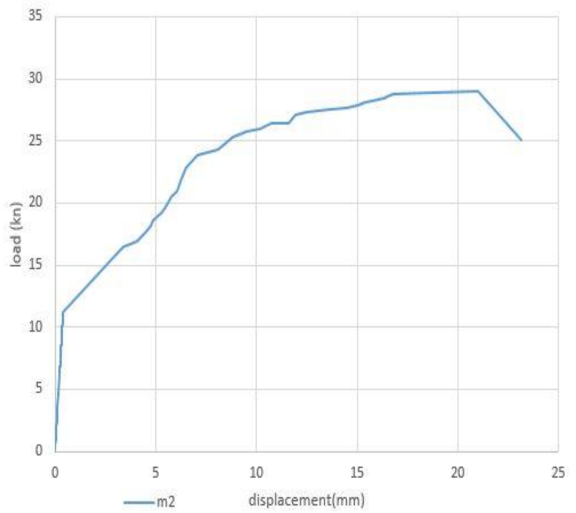

(G) Using one layer of CFRP around beam

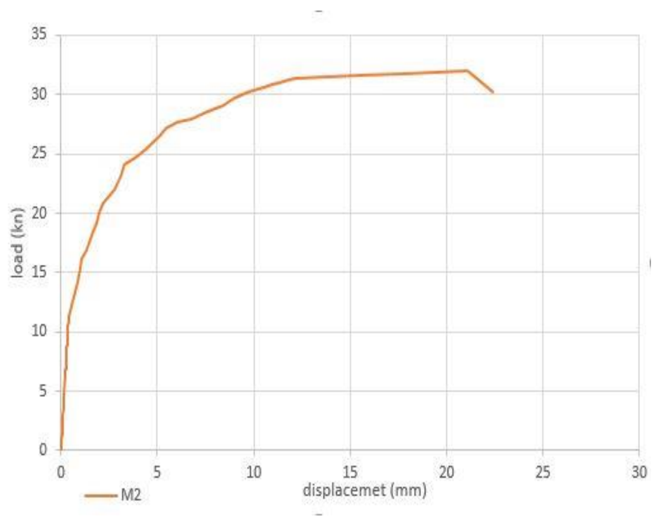

(H) using two-layer of CFRP around the column

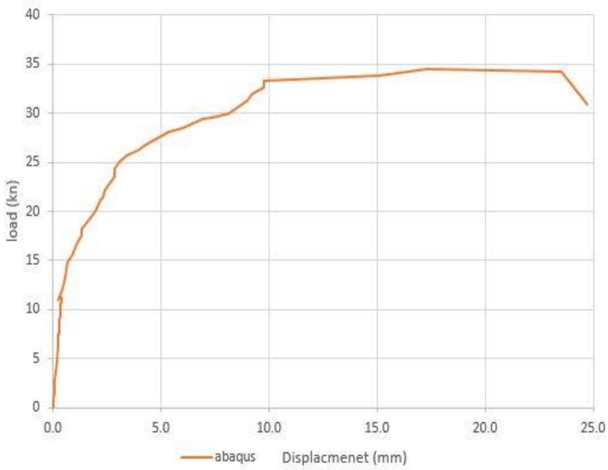

(I) using three-layer of CFRP

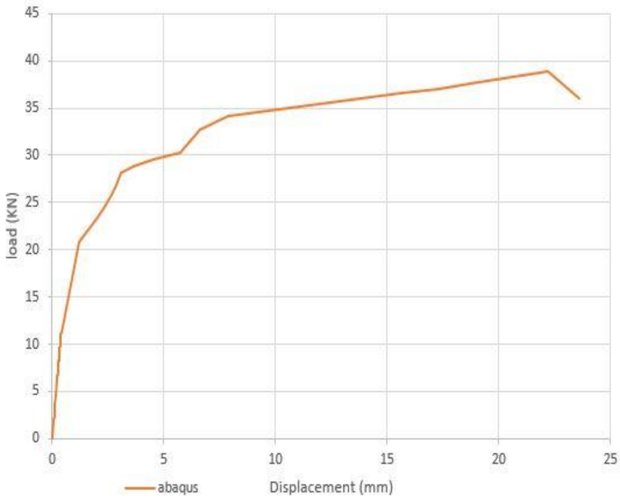

(J) using four-layer of CFRP

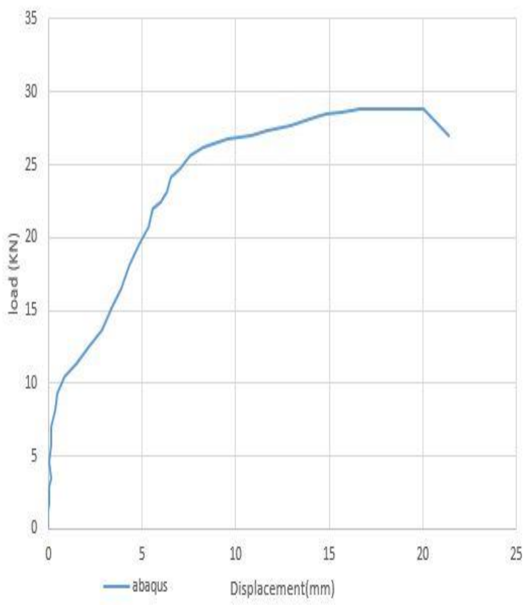

(K) Using two-layers of CFRP

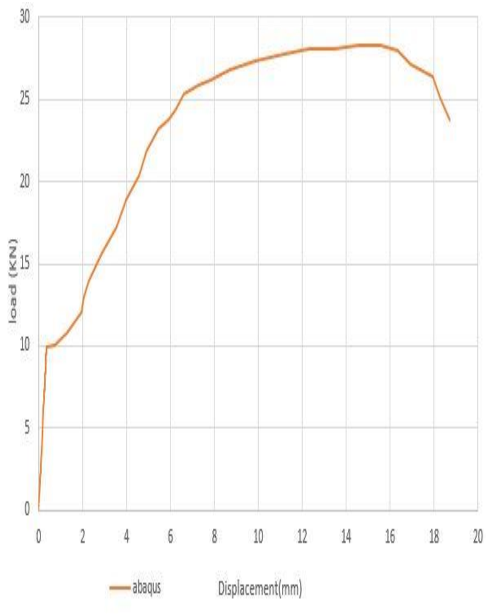

(L) using one layer of CFRP and fc=67 MPa

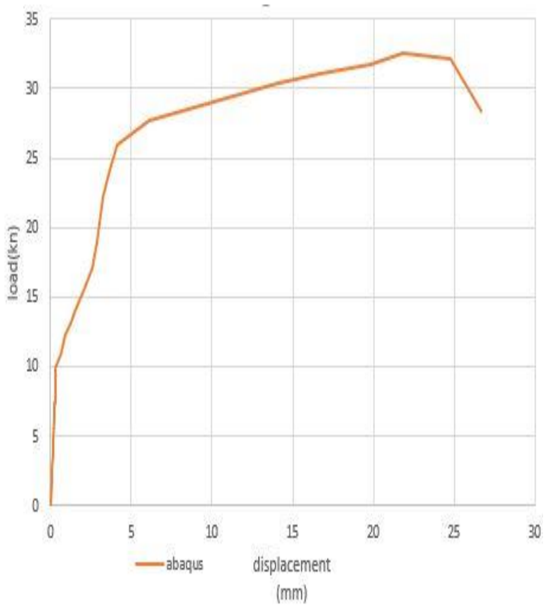

(M) Using three layers of CFR

4. Conclusion

Based on the results of the finite element study conducted using ABAQUS software, the following conclusions can be drawn: Mesh convergence studies were conducted to determine a suitable mesh size that would lead to a close agreement with the experimentally observed response. Four sizes of the element, namely 50 mm,30 mm,20mm and11 mm were initially adopted as a uniform mesh size. The results showed that the element's size significantly affects the hysteresis curve behavior. In this study, FE analysis results for the 20mm for model one and11 mm elements for model two size gave a better prediction. The similarity of the hysteresis curve resulted in the FE analysis using the 11 mm element's size compared to that gained from the experiment; this suggested a reasonably good agreement between the experimental observation and the prediction result from the FE analysis. And the FE models developed using ABAQUS were able to predict the failure mode, the overall response throughout the entire loading history, and the dissipated energy successfully, as they closely matched the respective experimental result. The FE models showed a good prediction of load-displacement envelope curves but did not predict well the stiffness degradation under uniaxial loading. effect of three key parameters on the structural response of strengthened joints was investigated. The key parameters considered were the concrete's compressive strength, the C FR, P, and the using HSC; their effect on the joints' shear strength was also considered. And the joint's strength changes with the variation of the beam's axial load. For a sample one from (55 Mpa, 65 MPa, 70 MPa, and

80 MPa), and affected for increasing the strength of joint due to applied load but decreasing ductility without using CFRP. Also the axial load had a favorable effect on both the joints' first crack and maximum joint shear stress.

Declaration of Competing Interest: The authors declare that they have no conflict of interest.

References

[1] Y.B.A.Tahnat, "effect of using CFRP wraps on the strength and ductility behaviors of the exterior reinforced concrete joint," *composite structure,* vol. 201, no. 2018, pp. 721-739, 2018.

[2] T. A. B.G.Charalambidi, "fatigue behavior of large-scale reinforced concrete beams strengthened in flexture with fiber-reinforced polymer laminates," *Journal of composites for construction,* vol. 20, no. 2, p. 5, 2016.

[3] C. a. M.Golias, "Full-scale tests of RC joints with minor to moderate seismic damage repaired using C-FRP sheets," *earthquake and structures,* vol. 15, no. 3, pp. 617-627, 2018.

[4] P. a. B.Li, "High-strength concrete exterior beam-column joints with high-yield strength steel reinforcements," *Eng.structure,* vol. 145, no. 4, pp. 305-321, 2017.

[5] Kakaletsis, D.J., David, K.N. and Karayannis, C.G., 2011. Effectiveness of some conventional seismic retrofitting techniques for bare and infilled R/C frames. Structural Engineering and Mechanics, 39(4), pp.499-520.

[6] Karayannis, C.G., 2015. Mechanics of external RC beam-column joints with rectangular spiral shear reinforcement: experimental verification. Meccanica, 50(2), pp.311-322.

[7] Fahmy, M.F., Farghal, O.A. and Sharobeem, G.F., 2018. Exploratory study of adopting longitudinal column reinforcement details as a design-controllable tool to seismic behavior of exterior RC beam-column joints. Engineering Structures, 174, pp.95-110.

[8] Y. a. C. L.Tong Y.Chen, "Cyclic behavior of beam-to-column joints with cast steel connectors," *j.constr.steel Res.,* vol. 116, no. 8, pp. 114-130, 2016.

[9] A. M. B. a. X.Liu, "Experimental study of flush endplate beam-to-column composite joints with precast slabs and deconstruct able bolted shear connectors," *structures,* vol. 7, no. 9, pp. 43-58, 2016.

[10] S. A. a. M. Marefat, "Seismic retrofit of external RC beam-column joints by joint enlargement using prestressed steel angles," *Eng. Struct,* vol. 81, no. 10, pp. 265-288, 2014.

[11] H. T. a. H.Park, "Design considerations for interior RC beam-column joints with additional bars," *engineering structures,* vol. 98, no. 11, pp. 1-13, 2015.

[12] Z. W. Suyan Wang, "Experimental Investigation of Ductility of Reinforced High Strength Concrete T-section Beams Retrofitted with CFRP," *advanced material research,* vol. 449, no. 12, pp. 601-610, 2012.

[13] Tran, M.T., 2016. Influence factors for the shear strength of exterior and interior reinforced concrete beam-column joints. Procedia engineering, 142, pp.63-70.

[14] U. Akguzel, Seismic Performance of FRP Retrofitted Exterior RC Beam-Column Joints under Varying Axial and Bidirectional Load-ing, in Civil and Natural Resources Engineering, Australia: University of canterbury, 2011.